The p53 regulatory gene *MDM2* is a direct transcriptional target of MYCN in neuroblastoma

Andrew Slack*, Zaowen Chen*, Roberto Tonelli†, Martin Pule*, Lisa Hunt*, Andrea Pession†, and Jason M. Shohet*‡

*Center for Cell and Gene Therapy, Texas Children's Cancer Center, Baylor College of Medicine, 1102 Bates Street, Houston, TX 77030, and †Department of Pediatrics, University of Bologna, Santa Orsola Hospital, Via Massarenti, 11-40138 Bologna, Italy

Edited by Robert N. Eisenman, Fred Hutchinson Cancer Research Center, Seattle, WA, and approved November 19, 2004 (received for review July 28, 2004)

The *MYCN* oncogene is the major negative prognostic marker in neuroblastoma with important roles in both the pathogenesis and clinical behavior of this aggressive malignancy. *MYC* oncogenes activate both proliferative and apoptotic cellular pathways and, accordingly, inhibition of p53-mediated apoptosis is a prerequisite for MYC-driven tumorigenesis. To identify novel transcriptional targets mediating the MYCN-dependent phenotype, we screened a MYCN-amplified neuroblastoma cell line by using chromatin immunoprecipitation (ChIP) cloning. We identified the essential p53 inhibitor and protooncogene *MDM2* as a putative target. MDM2 has multiple p53-independent functions modulating cell cycle and transcriptional events. Standard ChIP with MYCN antibodies established the binding of MYCN to a consensus E-box within the human *MDM2* promoter. Oligonucleotide pull-down assays further established the capacity of MYCN to bind to this promoter region, confirming the ChIP results. Luciferase reporter assays confirmed the E-box-specific, MYCN-dependent regulation of the *MDM2* promoter in MYCN-inducible neuroblastoma cell lines. Real-time quantitative PCR and Western blot analysis demonstrated a rapid increase in endogenous *MDM2* mRNA and MDM2 protein upon induction of MYCN. Targeted inhibition of MYCN in a *MYCN*-amplified neuroblastoma cell line resulted in decreased MDM2 expression levels with concomitant stabilization of p53 and induction of apoptosis. Our finding that MYCN directly modulates baseline MDM2 levels suggests a mechanism contributing to the pathogenesis of neuroblastoma and other MYC-driven malignancies through inhibition of MYC-stimulated apoptosis.

oncogene | transactivation | apoptosis | pediatric cancer | chromatin immunoprecipitation

Metastatic neuroblastoma is a remarkably aggressive pediatric malignancy. Despite recent intensive escalation of therapy, only marginal therapeutic gains have been made (1), and improvement in outcome clearly requires a better understanding of the pathogenesis and pathophysiology of this disease. The *MYCN* oncogene is amplified in 25% of neuroblastomas and is the most powerful clinical prognostic marker for poor survival (2). Tissue-targeted expression of *MYCN* is sufficient to induce neuroblastoma in transgenic mice (3), suggesting this oncogene plays an important role in the pathogenesis of neuroblastoma. *In vitro* studies demonstrate that MYCN overexpression induces an aggressive phenotype with decreased contact inhibition, decreased growth factor dependence, and increased metastatic potential (4, 5). These findings correlate with the malignant clinical behavior of *MYCN*-amplified tumors in children.

MYCN is a transcription factor with well defined mechanisms of both transcriptional activation, when bound to promoter E-boxes as a MYCN/Max heterodimer, and transcriptional repression, when bound as a heterodimer with Mnt, Mxi, Mad, or other negative cofactors (6, 7). MYCN is involved in many aspects of normal and oncogenic cellular physiology, including proliferation, cell cycle regulation, apoptosis, and genomic instability (8, 9). Clinically and therapeutically relevant insight into neuroblastoma biology thus can be achieved through identification of the downstream transcriptional targets of MYCN involved in these pathways.

In vitro studies of neuroblastoma cell lines demonstrate that overexpression of MYCN induces the conflicting cellular processes of rapid proliferation and apoptotic cell death (10). MYCN shortens the G_1–S phase transition, increases cell proliferation rates, and decreases cell dependence on paracrine growth factors (5, 11, 12). Concurrently, MYCN suppresses Bcl-2, activates Bax, and sensitizes cells to genotoxicity-mediated apoptosis through intrinsic apoptosis pathways (13). MYCC has been shown to activate the ARF tumor suppressor, leading to p53 activation and apoptosis through Bcl-x and Bcl-2-dependent and -independent pathways (14). Less than 2% of neuroblastomas have mutated p53, and the p53 pathways are functionally active in the majority of *de novo* tumors (15, 16). Therefore, for MYCN-expressing neuroblastoma precursor cells to escape p53-mediated cell death, proliferate, and progress to invasive malignancy, a balance must be struck between MYCN-driven proliferation and MYCN-driven apoptosis.

In this study we use chromatin immunoprecipitation (ChIP), transcriptional reporter assays, oligonucleotide pull-down assays, quantitative RT-PCR, and Western blot analysis to screen for novel transcriptional targets of MYCN. We demonstrate direct transcriptional regulation of *MDM2* by MYCN in neuroblastoma. We further demonstrate, through targeted inhibition of MYCN, that MYCN-dependent transactivation of *MDM2* might prevent p53-stimulated apoptosis in a MYCN-amplified cell line. Our experiments argue strongly that increased constitutive transcriptional activation of *MDM2* by MYCN contributes to MYCN-driven oncogenesis by providing proproliferative counterbalance to MYC-dependent apoptotic sensitization.

Methods

Antibodies. Anti-MDM2 (Oncogene), anti-MYCN (Becton Dickinson Pharmingen), anti-p53 (Santa Cruz Biotechnology), anti-α-tubulin (Santa Cruz Biotechnology), and anti-actin (Sigma) mAbs and horseradish peroxidase-conjugated goat anti-mouse antibody (Sigma) were used for ChIP and Western blot analysis as described.

Plasmids. An 898-bp fragment of the *MDM2* promoter was inserted into the pGL3-Basic plasmid upstream of the luciferase reporter gene to construct *MDM2* luciferase WT. The E-box element at −481 bp was mutated from CACGTG to CAGG by using overlapping primer mutagenesis to construct the *MDM2* luciferase mutant reporter plasmid (primer sequences are in *Supporting Text,* which is published as supporting information in the PNAS web site).

This paper was submitted directly (Track II) to the PNAS office.

Abbreviations: ChIP, chromatin immunoprecipitation; PNA, peptide nucleic acid.

‡To whom correspondence should be addressed. E-mail: jmshohet@texaschildrenshospital.org.

Tissue Culture and Cell Lines. All cell lines were maintained in RPMI media 1640 (Invitrogen) supplemented with 10% Tet-approved FBS (Invitrogen), penicillin, and streptomycin. Manfred Schwab (University of Heidelberg, Heidelberg) provided the Tet21 MYCN-inducible cell line. MYCN-2 and MYCN-3 cell lines were generated as follows: the MYCN cDNA was cloned into the pTRE2-Hygro vector (BD Biosciences) containing a tetracycline-responsive promoter. This construct was then transfected into a SHEP subclone stably expressing the TRE-response element and selected with hygromycin. The JF *MYCN*-amplified neuroblastoma cell line was obtained from Malcolm Brenner (Baylor College of Medicine).

Transfections and Luciferase Reporter Assay. Approximately 1.0×10^5 cells were transfected with 1 μg of reporter plasmid. Cells were transfected with Geneporter (Gene Therapy Systems, San Diego) over 4 h in serum-free media. Luciferase reporter activity was measured by using the Luciferase Assay System (Promega) 48 h posttransfection. Protein lysate concentrations were used to normalize data.

Peptide Nucleic Acid (PNA) Design and Treatment. An antigene PNA homologous to a unique sequence of the noncoding (antisense) strand of *MYCN* exon 2 (base pairs 1650–1665: 5′-atgccgggcatgatct-3′; GenBank accession no. M13241) was used. A mismatched PNA (PNA_{mut}) containing three mismatch base substitutions (5′-**g**tgccg**a**gcatg**g**tct-3′) was used as a control (mismatches in bold). The PNAs were covalently linked to a C-terminus NLS peptide (PKKKRKV) to mediate transfer across the nuclear membrane (17). IMR-32 cells were treated with PNA inhibitors at 10 μM (or without, control) in serum-free medium for 6 h, followed by addition of complete medium.

Cytofluorometric Apoptosis Analysis. FACS analysis with FITC-conjugated annexin V (BD Biosciences) was performed in IMR-32 cells 24 h after 10 μM PNA, PNA_{mut}, and control were added according to the manufacturer's protocol.

Real-Time PCR. Genomic DNA from ChIP analysis and RNA were quantified by real-time PCR using the Opticon Monitor (MJ Research, Cambridge, MA) (see *Supporting Text* for complete primer sequences and methods). Five microliters of ChIP DNA was used as template for ChIP PCR studies. One hundred nanograms of RNA was used as template for RT-PCR. QuantiTect SYBR Green (Qiagen, Valencia, CA) PCR mixes were used for PCR.

Western Blot Analysis. Cells were lysed in prewarmed (95°C) cell lysate buffer (2% SDS/300 mM Tris·Cl, pH 6.8/10% glycerol), boiled 10 min, and sonicated with four 5-s pulses. Samples then were cleared by centrifugation ($13,000 \times g$ for 5 min) and diluted in loading buffer for analysis. Equal amounts of protein were separated by SDS/PAGE on 7.5% gels, transferred to poly(vinylidene difluoride) membrane (Amersham Pharmacia), and incubated with antibodies. Immunoblots were then visualized by using the enhanced chemiluminescent system (Amersham Pharmacia).

Biotin-Streptavidin Pull-Down Assay. Transcription factor pull-down assays were done as described (18). Briefly, two double-stranded oligonucleotides corresponding to positions −388 to −364 of the human *MDM2* P2 promoter and containing biotin on the 5′ nucleotide were incubated with 200 μg of JF cell nuclear lysate for the pull-down assays (see *Supporting Text* for details). MYCN was detected as described in Western blot analysis.

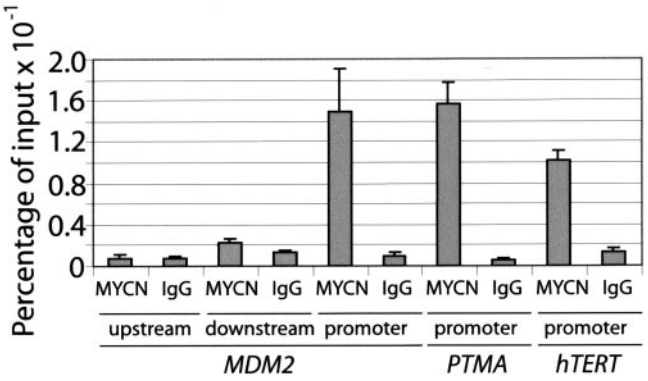

Fig. 1. ChIP of the *MDM2* promoter by the MYCN antibody. Real-time PCR was used to evaluate the precipitation of E-box *MDM2* promoter and upstream and downstream region fragments from JF cell line chromatin by using an anti-MYCN mAb (MYCN). MYCN-responsive promoters of prothymosin-α (*PTMA*) and telomerase reverse transcriptase (*hTERT*) also were evaluated. Relative enrichment was calculated by comparison to the threshold cycle (C_T) value for input genomic DNA and plotted as a percentage of input. Control immunoprecipitations using an isotype-matched antitubulin antibody control (IgG) are also plotted for comparison. Error bars plotted represent mean values ± SE of triplicate measurements from three independent experiments.

ChIP. ChIP cloning was performed with lysates of the JF *MYCN*-amplified neuroblastoma cell line. Using a modified version of published protocols (19, 20), we performed two rounds of immunoprecipitation with an anti-MYCN mAb. A representative plasmid library of the resulting pool of putative MYCN targets was generated by *Dpn*II restriction digestion and PCR linker ligation, followed by limited PCR amplification (22 cycles) generating sufficient material for cloning into a TOPO-TA vector. Clones were sequenced and localized on the human genome with the BLAT search function of the University of California, Santa Cruz genome browser (http://genome.ucsc.edu).

For standard ChIP assays we fixed and prepared lysates from 1.0×10^7 log-phase JF neuroblastoma cells essentially as described (21). Anti-MYCN and antitubulin antibodies were used for immunoprecipitation. The following primer pairs were used for *MDM2* ChIP: *MDM2* promoter region, intron 1 (forward, 5′-agcctttgtgcggttcgtg-3′; reverse, 5′-cccccgtgacctttaccctg-3′), *MDM2* region 15.9 kb upstream (forward, 5′-acagaacagcacatggccaggata-3′; reverse 5′-gaggctgtacctgcagtgtaatag-3′), and *MDM2* region 13.3 kb downstream (forward, 5′-cctgcttgaagtgcagtggtaatc-3′; reverse 5′-aggccgaggtgagaatatctcttg-3′).

Results

ChIP Cloning and Identification of *MDM2* as a Transcriptional Target of MYCN. To identify novel transcriptional targets of MYCN we generated a library of MYCN-associated promoters by using ChIP and linker-specific PCR-based cloning (see *Methods*). Analysis of 128 clones revealed matches to 51 known genes and 33 predicted genes (unpublished data). One clone was an exact match to the first intron of *MDM2*.

Closer analysis revealed an E-box at position −381 relative to the first base of the second exon of *MDM2*. We then confirmed our screening result by performing standard ChIP with the same anti-MYCN antibody, using PCR primers that flanked the E-box element in the *MDM2* promoter. We could specifically enrich ≈15-fold for the *MDM2* E-box region with the MYCN antibody relative to an isotype-matched control antibody as measured by real-time quantitative PCR (Fig. 1). We also examined regions upstream and downstream of the *MDM2* promoter and could not demonstrate enrichment relative to an isotype control antibody for these regions. Recoveries and enrichment relative to isotype

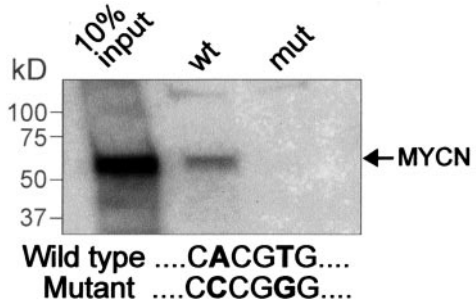

Fig. 2. Oligonucleotide pull-down assay with Western blot for MYCN transcription factor. Biotinylated double-stranded 24-mer oligonucleotides homologous to the *MDM2* promoter region containing the second intron E-box were incubated with JF cell lysates as described. Immobilized streptavidin was used to precipitate the oligonucleotide/transcription factor complexes. These were separated on SDS/PAGE, and a representative anti-MYCN Western blot is shown. A mutated oligonucleotide control (mut) shows no MYCN-specific signal, suggesting that MYCN binding is E-box-dependent. This experiment was repeated three times with independently generated cell lysates, and consistent results were obtained. Control isotype-matched antibodies were used for Western blotting and showed no evidence of nonspecific signals in pull-down lanes.

control immunoprecipitation for established MYCN-responsive promoters of prothymosin-α and telomerase (22) are very similar to those observed for *MDM2* (Fig. 1). Gel electrophoresis and melting curve analysis demonstrated unique, well defined PCR products for all primer sets used (data not shown).

MYCN Binds the E-Box Element of the *MDM2* Promoter *in Vitro*. To assess direct binding of MYCN to the *MDM2* promoter E-box, we performed transcription factor pull-down assays with double-stranded oligonucleotides and neuroblastoma cell lysates (as described in ref. 18). This method uses streptavidin beads to precipitate biotin-labeled double-stranded oligonucleotides homologous to the promoter element of interest and any associated DNA binding transcription factors. A 24-mer oligonucleotide homologous to the *MDM2* promoter spanning the E-box identified by ChIP (positions −388 to −364) was incubated with nuclear lysates of the JF cell line, and the resulting complexes then were precipitated with streptavidin beads. SDS/PAGE and Western blotting of the resulting pull-down material then were performed. As illustrated in Fig. 2, we could reproducibly demonstrate the association of MYCN with the oligonucleotide containing WT E-box sequence but not with a mutated E-box oligonucleotide control. Identical Western blots probed with unrelated isotype-matched antibodies exhibited no specific signal in the pull-down lanes (data not shown). This experiment provides additional *in vitro* data confirming the association of MYCN with the *MDM2* promoter found in our ChIP experiments, strongly suggesting that MYCN binds directly with the E-box element in the *MDM2* promoter.

***MDM2* Promoter Reporter Constructs Are Responsive to MYCN.** To determine whether MYCN binding to the *MDM2* E-box activates transcription of the *MDM2* gene we performed luciferase reporter assays. The *MDM2* gene is transcribed under the control of two distinct promoters (P1, upstream of exon 1 and P2, between exon 1 and exon 2) (23). The P1 promoter is constitutively active at a low level, whereas the inducible P2 promoter contains multiple transcription factor binding sites, including those for p53 and Ets, in addition to the consensus E-box (24). Transcription from the P2 promoter is rapidly up-regulated by active p53 (23). To explore the relationship between expression of MYCN and *MDM2* transactivation, we constructed a luciferase reporter construct containing the human *MDM2* P2 promoter (Fig. 3*A*). This promoter fragment

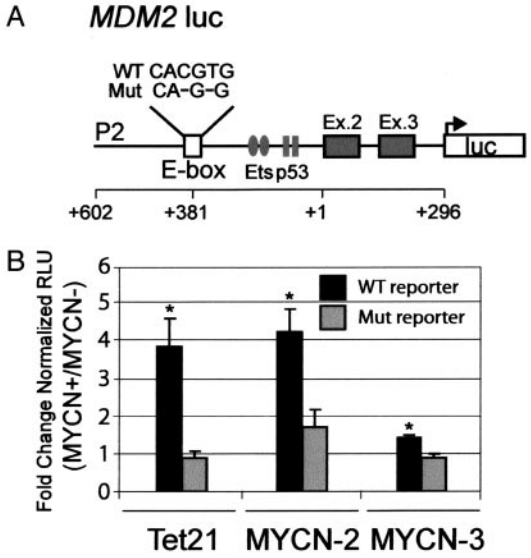

Fig. 3. Luciferase reporter assays demonstrate activation of the *MDM2* promoter. *MDM2* luciferase reporter constructs (*MDM2* luc) containing WT and mutant (Mut) E-box elements were cloned as described in *Methods*. (*A*) Schematic of *MDM2* promoter construct. (*B*) Transient transfection of MYCN-inducible cell lines (Tet21, MYCN-2, and MYCN-3) demonstrates MYCN-dependent transactivation of the WT reporter construct but no significant response to MYCN induction with the mutant reporter construct. Fold change in activity for WT and mutant constructs [relative luciferase units (RLU) ± SE] after induction is plotted relative to noninduction. All transfections were performed in triplicate and repeated at least three times with similar results. * indicates statistical significance as determined by paired *t* test ($P < 0.01$ for Tet 21, $P < 0.02$ for MYCN-2, and $P = 0.05$ for MYCN-3).

includes the minimum region required for maximal luciferase reporter activity as compared with other deletion mutants (25). A specific two-base deletion within the E-box element was introduced into a mutated reporter construct as a control. The *MDM2* luciferase constructs then were introduced into three different *MYCN*-inducible cell lines derived from the parental neuroblastoma cell line SHEP: Tet21, a previously described Tet-off subclone (5) and the MYCN-2 and MYCN-3 Tet-on clones isolated in our laboratory. All of these lines rapidly up-regulate MYCN expression upon induction (removal or addition of tetracycline, for Tet-off and Tet-on clones, respectively) as demonstrated by quantitative RT-PCR and Western blot (data not shown). We found that MYCN induction resulted in a consistent and statistically significant increase in *MDM2* transactivation when the WT reporter construct was used. In contrast, no MYCN-responsive increase was observed with the mutant E-box construct (Fig. 3*B*).

MYCN Induction Increases Endogenous MDM2 Levels in Neuroblastoma. Next, we assessed MYCN-dependent changes in endogenous *MDM2* mRNA and MDM2 protein levels in the *MYCN*-inducible cell lines. Western blot analysis for MDM2 demonstrates a 1.5- to 2.5-fold increase in MDM2 protein after MYCN induction (Fig. 4 *A* and *B*). In these cell lines, MYCN protein levels are maximal between 12 and 16 h after induction (data not shown and ref. 5). We measured *MDM2* mRNA levels by using quantitative real-time PCR (comparative C_T method) in RNA isolated from *MYCN*-induced and noninduced cell lines. We found a 2.8- to 3-fold increase in *MDM2* message levels after 24 h of MYCN induction (Fig. 4*B Left*). Kinetics of MYCN induction as analyzed by Western blot demonstrate rapid elevation of MDM2 protein levels upon induction of MYCN (Fig. 4*C*). Our data demonstrate that increases in MDM2 protein

GENETICS

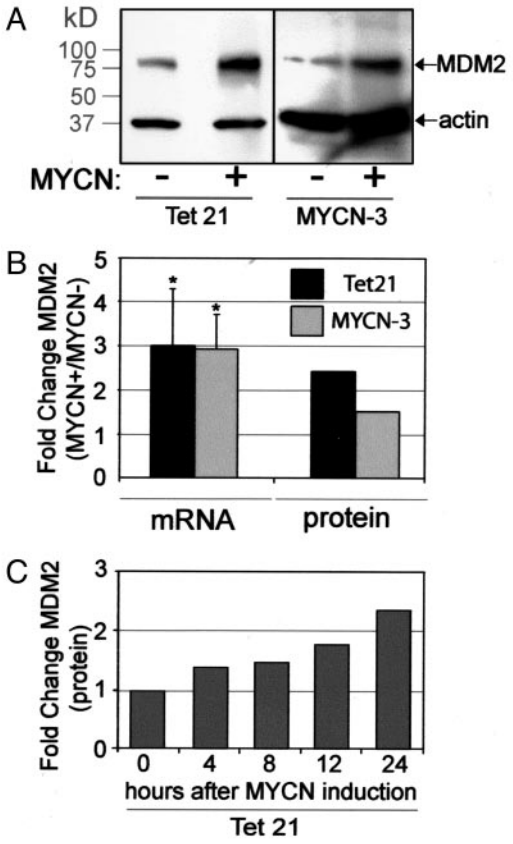

Fig. 4. MYCN regulates endogenous *MDM2* mRNA and MDM2 protein levels. (*A*) Representative Western blots of MDM2 in Tet 21 and MYCN-3 cell lines after 24 h of MYCN induction. (*B*) Quantification of relative change in mRNA and protein levels in Tet 21 and MYCN-3 cell lines after 24 h of MYCN induction. Real-time PCR data were normalized to GAPDH, and fold increase in *MDM2* mRNA expression was calculated by the comparative C_T method from the means of triplicate PCRs. Protein expression was quantified digitally on a Kodak 2000R Image Station and normalized to actin level to account for gel-loading differences. * indicates statistical significance as determined by *t* test ($P < 0.05$). (*C*) Protein was extracted from Tet21 cells, harvested at various times postinduction, and processed as above. MDM2 signal was normalized to actin as above. Each experiment was independently repeated three times with similar results.

correlate with *MDM2* mRNA levels and suggest that MYCN increases MDM2 levels through elevated transcription.

MYCN Inhibition Leads to Decreased MDM2, Increased p53, and Apoptosis. To determine the functional consequences of MYCN inhibition on MDM2 and its effectors, we treated the *MYCN*-amplified IMR-32 neuroblastoma cell line with a PNA inhibitor targeted to the second exon of MYCN (17, 26). PNAs are DNA analogs with the sugar-phosphate backbone replaced by a peptide polymer and thus are highly resistant to nuclease or protease degradation (27, 28). PNAs are rapidly taken up by neuroblastoma cells, permitting us to overcome the poor transfection efficiency of neuroblastoma cell lines (17).

As shown, MYCN expression levels are dramatically diminished at 12 h (Fig. 5*A*) and are undetectable 24 h after PNA treatment (17). Western blot also demonstrates dramatically reduced MDM2 protein levels at 12 h after treatment. In addition, real-time PCR demonstrates a decrease in *MDM2* mRNA levels of ≈16-fold at the same time point (Fig. 5*B*). No significant effects on *MDM2* expression were observed for PNA_{mut}-treated cells relative to control. We then asked whether

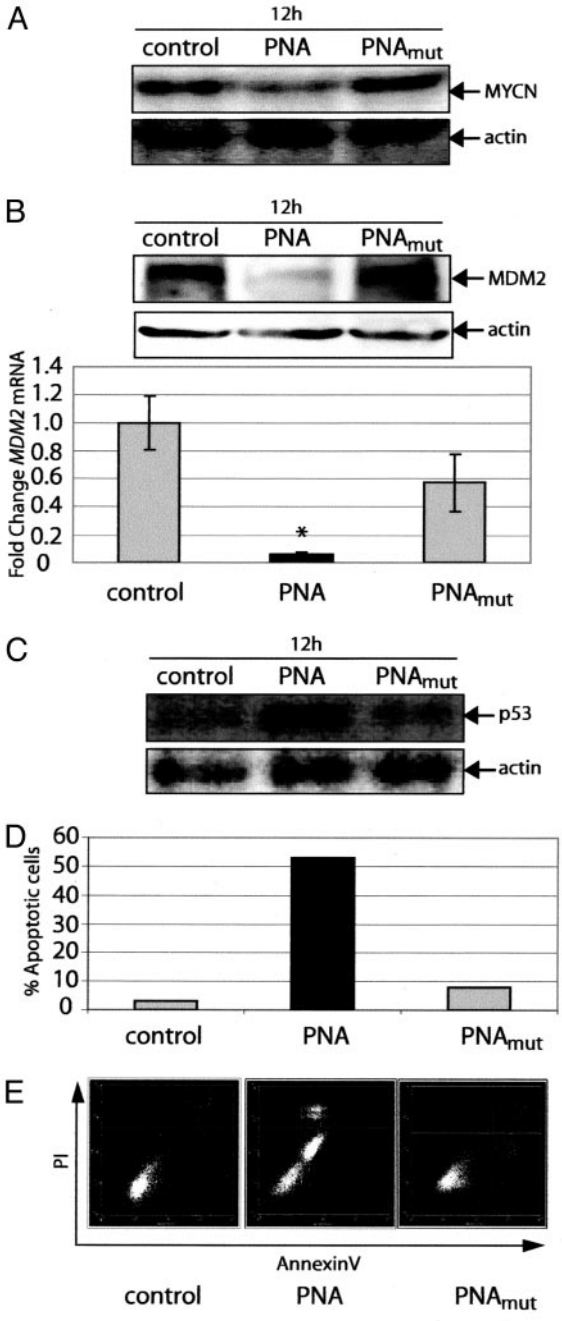

Fig. 5. Anti-MYCN-targeted PNA down-regulates MDM2 and induces apoptosis. (*A–C*) Western blot analysis of protein extracted from control, PNA-treated, and PNA_{mut}-treated IMR-32 cells harvested 12 h after treatment is shown. Extracts were separated on SDS/PAGE and probed with antibodies to MYCN (*A*), MDM2 (*B*), and p53 (*C*). Blots were reprobed with actin and signals normalized as in Fig. 4. Quantitative PCR for *MDM2* was also performed as above and demonstrated a clear difference in mRNA levels concordant with the observed decrease in protein (*B*). Data are plotted as fold change relative to control-treated cells. * indicates statistical significance as determined by independent samples *t* test ($P < 0.03$) PNA vs. PNA_{mut}. (*D* and *E*) Apoptosis was assessed by annexin V staining after 24 h with results plotted in *D*, and representative FACS plots used for quantitation shown in *E* [the annexin signal is plotted on the *x* axis, and the propidium iodide (PI) signal is plotted on the *y* axis].

this reduction in MDM2 could result in the stabilization of p53, and consequently, in increased cell death. Indeed, we observed increased p53 protein levels at 12 h in the PNA-treated cells that

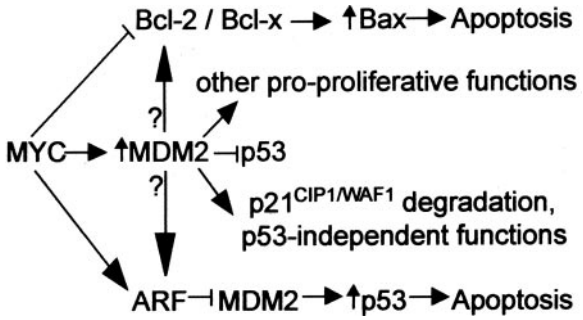

Fig. 6. MYC-dependent apoptotic pathways. MYC activates ARF and inhibits Bcl family members, leading to apoptosis. MDM2 can counteract these influences by the inhibition of p53, leading to deficient cell cycle arrest and apoptosis. MDM2 has p53-independent functions that might alter the BAX and ARF pathways without altering p53.

were not observed in the PNA_{mut}-treated cells (Fig. 5*C*). Consistent with this observation, 53% of PNA-treated cells were apoptotic as compared with 8% in PNA_{mut} after 24 h of PNA treatment as measured by annexin V staining (Fig. 5 *D* and *E*). These data suggest that MYCN-driven expression of *MDM2* might be in part responsible for maintaining MDM2 expression levels sufficient to destabilize p53 and prevent apoptosis in MYCN-amplified neuroblastoma.

These data suggest that MYCN, through direct transactivation of *MDM2*, can overcome the normally tight control of MDM2 expression in neuroblastoma cells. As discussed below, MDM2 is overexpressed in many types of malignancies and contributes to inhibition of p53 regulation of cell cycle progression and apoptosis in the presence of stress in other tumor models. We present the hypothesis that MYCN-driven aberrant expression of MDM2 alters the biology of neuroblastoma precursors, contributing to the MYCN-driven pathogenesis of this disease.

Discussion

Our results demonstrate direct regulation of MDM2 expression by MYCN and suggest a pathogenic role for MDM2 in neuroblastoma. The primary function of MDM2 in normal cells is to inhibit p53 activity. It causes the degradation and nuclear export of p53 and interferes with p53 transcriptional activity (29). It is a direct transcriptional target of p53 and is rapidly up-regulated upon p53 activation, leading to feedback inhibition of p53 effects (reviewed in ref. 30). MDM2 has multiple p53-independent functions (31, 32) and participates in many of the same cellular pathways and processes mediated by the MYC family of oncoproteins, such as transcription (p300, NF-κ B, and SP1), differentiation (Numb and MyoD), and cell cycle regulations (p21, E2F/DP1, and pRB) (see refs. 32 and 33 and references therein). Additional p53-dependent and p53-independent functions of MDM2 continue to be discovered. It is not surprising that this highly active protein is tightly regulated by expression, protein/protein interactions, subcellular localization, and extensive post-translational modification in normal cells (32, 34). As a negative regulator of p53, MDM2 is considered a protooncogene, and its amplification and overexpression is documented in a wide variety of sarcomas, leukemias, and gliomas (reviewed in refs. 35 and 36). Our findings that MYCN can directly bind to the *MDM2* promoter, up-regulate baseline levels of MDM2, and inhibit p53-triggered apoptosis suggest an important pathogenic role for MDM2 in MYCN-driven neuroblastoma development.

Genetic studies demonstrate that the MYC family of oncoproteins, while driving proliferation, concurrently induce apoptotic signals through several distinct pathways (10, 13, 14). As illustrated in Fig. 6, MYC inhibits the antiapoptotic factors Bcl-2 and Bcl-x and activates Bax (37). MYC also indirectly activates ARF (the alternative reading frame of $p16^{INK4A}$) (38). ARF binds MDM2, inhibiting its E3 ubiquitin ligase activity and sequestering MDM2 in the nucleolus. Sequestration leads to increased p53 levels and transcriptional activity (14). In support of this mechanism, genetic knockout studies have shown that MDM2 is required for maximal MYCC-driven lymphomagenesis (39).

Although direct regulation of MDM2 by MYCC has yet to be confirmed, it has been shown by ChIP that MYCC associates with the *MDM2* promoter E-box in an inducible B cell lymphoma cell line (40). Although MYCN and MYCC share large regions of amino acid homology (>80% in some exons; ref. 41) and some common transcriptional targets, there are major differences in tissue-specific expression and transactivation pathways between these two oncogenes (8, 42) Our findings of MYCN-regulated MDM2 expression might be pertinent to MYCC-driven malignancies as well.

Much information regarding these pathways is derived from the Eμ-*myc* transgenic mouse where MYCC is aberrantly overexpressed under the control of an Ig promoter (43). Lymphomas that develop in these mice have high rates of mutations in either *p53* (25%) or *Arf* (30%) (44). When Eμ-*myc* mice were crossed with $Bax^{-/-}$ and $Bax^{+/-}$ mice, the *p53* and *Arf* mutations were found to be mutually exclusive, suggesting the MYCN-induced apoptotic Arf/Mdm2 pathway is functionally distinct from the Bcl-2/Bax pathway (37). As expected, overexpression of Bax strongly inhibits *Myc*-driven lymphomagenesis (45). Mdm2 was overexpressed or amplified in 50% of the mouse lymphomas tumors regardless of *p53* or *Arf* mutation.

When Eμ-*myc* mice were crossed with *mdm2* haploinsufficient mice, lymphomagenesis was markedly impaired and the number of circulating immature B cells was dramatically reduced (43, 46). In this model, mdm2 deficit increased the pressure for *p53* mutations: *p53* mutation frequency in resulting tumors increased from 25% to 50%. The observation of these effects with *mdm2* haplo-insufficiency suggests that small changes in MDM2 levels can dramatically influence the p53 response *in vivo*. These data demonstrate the need to inhibit apoptotic pathways for the development of MYC-driven lymphomas and that MDM2 plays a crucial role in restraining p53-mediated apoptosis in these models (46).

Our finding that MYCN can directly and positively regulate MDM2 expression in neuroblastoma cells suggests an additional pathway modulating MYCN-directed apoptosis (Fig. 6), possibly counterbalancing the ARF/MDM2 and Bcl-2/Bax pathways. A direct transcriptional link between MYCN and *MDM2* leading to elevated baseline MDM2 protein levels might constitutively suppress p53 expression, raising the threshold for activation of p53 through cell stress or genotoxic damage. Recently, elevated MYCN expression has been shown to produce neuroblast hyperplasia in developing sympathetic ganglia in pTH-MYCN transgenic mice (47). Abnormal persistence of hyperproliferating neuroblasts correlates closely with neuroblastoma tumorigenesis in these mice. Elevated MDM2 could disrupt developmentally programmed p53-mediated apoptosis or other p53-independent pathways regulated by differentiation signals present within these developing ganglia. This imbalance would lead to proliferation and persistence of hyperplastic neuroblast cells, contributing to MYCN-driven tumorigenesis.

Direct assessment of the role of deregulated MDM2 expression in neuroblastoma development will require specific inhibition of MDM2 in *in vivo* model systems. Inhibiting the interaction between MDM2 and p53 with small molecule inhibitors or other means could effectively lead to increased p53 activity and cell death. Proof of this principle recently has been demonstrated with osteosarcoma xenograft models (48). Because the overwhelming majority of *de novo* neuroblastomas are p53 WT, this approach might be an effective future therapeutic strategy.

We thank Dr. Guillermina Lozano for advice and review of the manuscript and Dr. Roberto Corradini (Santa Orsola Hospital) for synthesis and supply of the anti-MYCN PNA. A.S. was supported by a fellowship from the Canadian Institute of Health Research. J.M.S. was supported by National Institutes of Health Grant KO-8 CA90517-02 and grants from the Logenbaugh Foundation and Hope Street Kids Foundation.

1. Matthay, K. K., Villablanca, J. G., Seeger, R. C., Stram, D. O., Harris, R. E., Ramsay, N. K., Swift, P., Shimada, H., Black, C. T., Brodeur, G. M., *et al*. (1999) *N. Engl. J. Med.* **341,** 1165–1173.
2. Schwab, M. (2004) *Cancer Lett.* **204,** 179–187.
3. Weiss, W. A., Aldape, K., Mohapatra, G., Feuerstein, B. G. & Bishop, J. M. (1997) *EMBO J.* **16,** 2985–2995.
4. Schweigerer, L., Breit, S., Wenzel, A., Tsunamoto, K., Ludwig, R. & Schwab, M. (1990) *Cancer Res.* **50,** 4411–4416.
5. Lutz, W., Stohr, M., Schurmann, J., Wenzel, A., Lohr, A. & Schwab, M. (1996) *Oncogene* **13,** 803–812.
6. Grandori, C., Cowley, S. M., James, L. P. & Eisenman, R. N. (2000) *Annu. Rev. Cell Dev. Biol.* **16,** 653–699.
7. Sakamuro, D. & Prendergast, G. C. (1999) *Oncogene* **18,** 2942–2954.
8. Nesbit, C. E., Tersak, J. M. & Prochownik, E. V. (1999) *Oncogene* **18,** 3004–3016.
9. Felsher, D. W. & Bishop, J. M. (1999) *Proc. Natl. Acad. Sci. USA* **96,** 3940–3944.
10. Hogarty, M. D. (2003) *Cancer Lett.* **197,** 173–179.
11. Fotsis, T., Breit, S., Lutz, W., Rossler, J., Hatzi, E., Schwab, M. & Schweigerer, L. (1999) *Eur. J. Biochem.* **263,** 757–764.
12. Schweigerer, L., Ledoux, D., Fleischmann, G. & Barritault, D. (1991) *Biochem. Biophys. Res. Commun.* **179,** 1449–1454.
13. van Noesel, M. M. & Versteeg, R. (2004) *Gene* **325,** 1–15.
14. Nilsson, J. A. & Cleveland, J. L. (2003) *Oncogene* **22,** 9007–9021.
15. Hosoi, G., Hara, J., Okamura, T., Osugi, Y., Ishihara, S., Fukuzawa, M., Okada, A., Okada, S. & Tawa, A. (1994) *Cancer* **73,** 3087–3093.
16. Vogan, K., Bernstein, M., Leclerc, J. M., Brisson, L., Brossard, J., Brodeur, G. M., Pelletier, J. & Gros, P. (1993) *Cancer Res.* **53,** 5269–5273.
17. Tonelli, R., Fronza, R., Purgato, S., Camerin, C., Bolgna, F., Alboresi, S., Franzoni, M., Corradini, R., Sforza, S., Faccini, A., *et al*. (2004) *Mol. Cancer Ther.*, in press.
18. Ragione, F. D., Cucciolla, V., Criniti, V., Indaco, S., Borriello, A. & Zappia, V. (2003) *J. Biol. Chem.* **278,** 23360–23368.
19. Wells, J. & Farnham, P. J. (2002) *Methods* **26,** 48–56.
20. Weinmann, A. S. & Farnham, P. J. (2002) *Methods* **26,** 37–47.
21. Morrison, A. J., Sardet, C. & Herrera, R. E. (2002) *Mol. Cell. Biol.* **22,** 856–865.
22. Mac, S. M., D'Cunha, C. A. & Farnham, P. J. (2000) *Mol. Carcinog.* **29,** 76–86.
23. Zauberman, A., Flusberg, D., Haupt, Y., Barak, Y. & Oren, M. (1995) *Nucleic Acids Res.* **23,** 2584–2592.
24. Brown, C. Y., Mize, G. J., Pineda, M., George, D. L. & Morris, D. R. (1999) *Oncogene* **18,** 5631–5637.
25. Phelps, M., Darley, M., Primrose, J. N. & Blaydes, J. P. (2003) *Cancer Res.* **63,** 2616–2623.
26. Pession, A., Tonelli, R., Fronza, R., Sciamanna, E., Corradini, R., Sforza, S., Tedeschi, T., Marchelli, R., Montanaro, L., Camerin, C., *et al*. (2004) *Int. J. Oncol.* **24,** 265–272.
27. Nielsen, P. E., Pellestor, F., Paulasova, P. & Koppelhus, U. (2005) *Methods Mol. Biol.* **288,** 343–358.
28. Pellestor, F. & Paulasova, P. (2004) *Eur. J. Hum. Genet.* **12,** 694–700.
29. Momand, J., Wu, H. H. & Dasgupta, G. (2000) *Gene* **242,** 15–29.
30. Moll, U. M. & Petrenko, O. (2003) *Mol. Cancer Res.* **1,** 1001–1008.
31. Zhang, Z., Wang, H., Li, M., Agrawal, S., Chen, X. & Zhang, R. (2004) *J. Biol. Chem.* **279,** 16000–16006.
32. Ganguli, G. & Wasylyk, B. (2003) *Mol. Cancer Res.* **1,** 1027–1035.
33. Deb, S. P. (2003) *Mol. Cancer Res.* **1,** 1009–1016.
34. Meek, D. W. & Knippschild, U. (2003) *Mol. Cancer Res.* **1,** 1017–1026.
35. Onel, K. & Cordon-Cardo, C. (2004) *Mol. Cancer Res.* **2,** 1–8.
36. Moore, L., Venkatachalam, S., Vogel, H., Watt, J. C., Wu, C. L., Steinman, H., Jones, S. N. & Donehower, L. A. (2003) *Oncogene* **22,** 7831–7837.
37. Eischen, C. M., Roussel, M. F., Korsmeyer, S. J. & Cleveland, J. L. (2001) *Mol. Cell. Biol.* **21,** 7653–7662.
38. Russell, J. L., Powers, J. T., Rounbehler, R. J., Rogers, P. M., Conti, C. J. & Johnson, D. G. (2002) *Mol. Cell. Biol.* **22,** 1360–1368.
39. Alt, J. R., Greiner, T. C., Cleveland, J. L. & Eischen, C. M. (2003) *EMBO J.* **22,** 1442–1450.
40. Fernandez, P. C., Frank, S. R., Wang, L., Schroeder, M., Liu, S., Greene, J., Cocito, A. & Amati, B. (2003) *Genes Dev.* **17,** 1115–1129.
41. Stanton, L. W., Schwab, M. & Bishop, J. M. (1986) *Proc. Natl. Acad. Sci. USA* **83,** 1772–1776.
42. Zimmerman, K. & Alt, F. W. (1990) *Crit. Rev. Oncog.* **2,** 75–95.
43. Adams, J. M., Harris, A. W., Pinkert, C. A., Corcoran, L. M., Alexander, W. S., Cory, S., Palmiter, R. D. & Brinster, R. L. (1985) *Nature* **318,** 533–538.
44. Eischen, C. M., Weber, J. D., Roussel, M. F., Sherr, C. J. & Cleveland, J. L. (1999) *Genes Dev.* **13,** 2658–2669.
45. Knudson, C. M., Johnson, G. M., Lin, Y. & Korsmeyer, S. J. (2001) *Cancer Res.* **61,** 659–665.
46. Eischen, C. M., Woo, D., Roussel, M. F. & Cleveland, J. L. (2001) *Mol. Cell. Biol.* **21,** 5063–5070.
47. Hansford, L. M., Thomas, W. D., Keating, J. M., Burkhart, C. A., Peaston, A. E., Norris, M. D., Haber, M., Armati, P. J., Weiss, W. A. & Marshall, G. M. (2004) *Proc. Natl. Acad. Sci. USA* **101,** 12664–12669.
48. Vassilev, L. T., Vu, B. T., Graves, B., Carvajal, D., Podlaski, F., Filipovic, Z., Kong, N., Kammlott, U., Lukacs, C., Klein, C., *et al*. (2004) *Science* **303,** 844–848.